Tribology International 92 (2015) 472–484

Contents lists available at ScienceDirect

Tribology International

journal homepage: www.elsevier.com/locate/triboint

# Investigation of the contact stiffness variation of linear rolling guides due to the effects of friction and wear during operation

H.T. Zou *, B.L. Wang

*Graduate School at Shenzhen, Harbin Institute of Technology, Harbin 150001, PR China*

ARTICLE INFO

*Article history:*
Received 24 January 2015
Received in revised form
28 June 2015
Accepted 7 July 2015
Available online 14 July 2015

*Keywords:*
Linear rolling guide
Contact stiffness
Thermal deformation
Wear

ABSTRACT

This study investigates the contact stiffness variation of linear rolling guides due to the effects of friction and wear during operation. The initial and final contact stiffness models were established. As a validation of the predicted varying stiffness, the experimental modal analysis was performed on a specialized linear guide system. The results show that the contact stiffness of linear guides decrease with the increase of running distance, and the entire stiffness decay could be divided into two distinct stages depending on how the thermal and wear effects influence the contact deformations of the balls at different running distances.



## 1. Introduction

With the rapid development of modern machine tools, the demand for high performance transmission systems is rapidly increasing in response to the trend of high-speed/high-precision machining. Currently, the linear rolling guide has been widely used in a variety of ultra-precise industrial machinery due to its high stiffness, low friction, and relatively good reliability, etc. While research studies have shown that about 60% of the total dynamic stiffness and about 90% of the total damping in a whole machine tool structure originate in the joints [1], which means that linear rolling guides served as the key component of many high-precision machine tools are crucial in improving their dynamic performance. The mechanical behavior of linear rolling guides strongly depends on the equivalent contact stiffness of the ball between raceways, however, it may gradually deviate from the original value due to the changes in preload under different operating conditions [2,3]. Such variation in the contact stiffness of linear guides may bring the mechanisms to vibrate at different frequencies [4–7], and then directly affect the dynamic performance of machine tools. Thus, it has become necessary to monitor and understand the contact stiffness characteristics of linear guides during operation, which will not only provide reliable stiffness feedback to further improve their mechanical behavior but also help to predict the dynamic behavior of machine tools more accurately.

There is a generally accepted concept that the contact stiffness of linear guides will gradually deviate from the initial value during operation, but few researchers focused on how they are affected by the operating conditions. Naturally, frictional heat induced thermal deformation of the linear guides is the primary factor can be supposed to explain such variation, because it may directly change the preload of the linear guide and affect its contact stiffness. However, as to the thermal issues on transmission systems, researches mainly focus on ball screws [8–13], little active research on the thermal behavior of modern linear guides has been discussed. Although some theoretical models of the sliding elliptical contact have been developed [14–17], they still have some difficulty in dealing with the contact stiffness variation of linear guides under complicated thermal conditions. In addition, the wear of linear guides is unavoidable over long periods of operation. Rolling/sliding frictions induced different wear types of abrasion, adhesion, and material fatigue will gradually deteriorate the initial preloads of linear guides during operation [18,19]. Therefore, the entire contact stiffness variation of linear guides cannot be explained by thermal effect alone. However, the study of such stiffness variation induced by the wear of linear guides is also limited. Tao et al. [20] presented a calculation model to predict the wear of linear guides under different loads and running distances, and the results showed that the wear displacement increased with the increase of running distance and external load. However, their study did not further quantify the relationships between the contact stiffness and the wear of linear guides under different operating conditions.

The research on contact stiffness variation of linear rolling guides during operation was not developed in previous studies. This paper aims to explain quantitatively how the contact stiffness

* Corresponding author. Tel.: +86 755 26032119; fax: +86 755 26033490.
*E-mail addresses:* zouhaitian945@gmail.com (H.T. Zou), wangbl@hitsz.edu.cn (B.L. Wang).

http://dx.doi.org/10.1016/j.triboint.2015.07.005
0301-679X/

of linear guides change with the combined effects of friction and wear. We first established the initial contact stiffness model to obtain the initial contact stiffness of linear guides by iterating the analytical equations which consider the flexibility of contact bodies. Then, FEM calculations were performed to determine the frictional heat induced thermal deformation of the carriage, and Archard wear theory was employed to obtain the wear of the carriage under different running distances. Further, the varying contact stiffness were obtained by the final contact stiffness model which was established based on the combined displacements induced by the preload, thermal deformation, and wear of the linear guide. Finally, we investigated the frequency characteristic variation of the test linear guide with vibration tests for the verification of the predicted stiffness variations which were obtained by the proposed contact stiffness models, and the related frequency expressions for the rigid-body natural vibration of linear guides were derived.

## 2. Initial contact stiffness of linear rolling guides

The contact stiffness of the linear rolling guide greatly depends on the equivalent contact stiffness of the ball between raceways. In this work, the contact stiffness of linear rolling guide is represented by the equivalent contact stiffness of the balls between raceways due to the direct and simple relationship between them.

### 2.1. Hertz contact analysis

In linear rolling guides, the contacts between balls and raceways are regarded as Hertzian contact type. Fig. 1 shows the geometry of the ball and the raceway grooves of the carriage and rail. From Hertz elastic contact theory, the relative displacements between the ball and the raceways of the carriage and rail $\delta_{b-r}$ and $\delta_{b-c}$ can be expressed as

$$\delta_{b-r}=\varepsilon_{b-r}P^{\frac{2}{3}},\quad \delta_{b-c}=\varepsilon_{b-c}P^{\frac{2}{3}} \tag{1}$$

where $P$ is normal load, $\varepsilon_{b-r}$ and $\varepsilon_{b-c}$ are the load–deflection factors of the two contacts, and they are given by

$$\varepsilon_{b-r}=\vartheta_{b-r}\left[\frac{3}{2\sum\rho_{b-r}}\left(\frac{1-\upsilon_b^2}{E_b}+\frac{1-\upsilon_r^2}{E_r}\right)\right]^{\frac{2}{3}}\frac{\sum\rho_{b-r}}{2},$$
$$\varepsilon_{b-c}=\vartheta_{b-c}\left[\frac{3}{2\sum\rho_{b-c}}\left(\frac{1-\upsilon_b^2}{E_b}+\frac{1-\upsilon_c^2}{E_c}\right)\right]^{\frac{2}{3}}\frac{\sum\rho_{b-c}}{2} \tag{2}$$

where $E_b$, $\nu_b$, $E_r$, $\nu_r$, $E_c$, and $\nu_c$ are the Young's modulus and Poisson's ratio of the ball, rail, and carriage, $\vartheta_{b-r}$ and $\vartheta_{b-c}$ are the coefficients which will be given later, $\sum\rho_{b-r}$ and $\sum\rho_{b-c}$ are the curvature sums of the rail and carriage. The radius of the curvatures of the ball and the raceway grooves of the carriage and rail in the principal plane *I* and plane *II* are, respectively, $r_{bI}$, $r_{bII}$, $r_{cI}$, $r_{cII}$, $r_{rI}$, and $r_{rII}$, as shown in Fig. 1. Here, $r_{bI}=r_{bII}=d_0/2$, $r_{cI}=r_{rI}=\infty$, $r_{cII}=-R_c$, $r_{rII}=-R_r$, where $d_0$ is the ball diameter, $R_c$ and $R_r$ are the raceway groove radius of the carriage and rail. The curvature sums for the rail and carriage are obtained as $\sum\rho_{b-r}=4/d_0-1/R_r$, $\sum\rho_{b-c}=4/d_0-1/R_c$.

From above, the total equivalent contact deformation of the ball between the rail and carriage $\delta$ is

$$\delta=\delta_{b-r}+\delta_{b-c}=\varepsilon P^{\frac{2}{3}} \tag{3}$$

and the equivalent load–deflection factor $\varepsilon$ is obtained as

$$\varepsilon=0.655\left[\vartheta_{b-r}\left(\frac{1-\upsilon_b^2}{E_b}+\frac{1-\upsilon_r^2}{E_r}\right)^{2/3}\left(\frac{4R_r-d_0}{R_rd_0}\right)^{1/3}+\vartheta_{b-c}\left(\frac{1-\upsilon_b^2}{E_b}+\frac{1-\upsilon_c^2}{E_c}\right)^{2/3}\left(\frac{4R_c-d_0}{R_cd_0}\right)^{1/3}\right] \tag{4}$$

When two elastic bodies with smooth curved surface come into contact, the contact area becomes elliptic. For the linear guides, the semi-major axis $a$ and semi-minor axis $b$ of the elliptic contact area, as shown in Fig. 1, are given by

$$a=\xi\left[\frac{3P}{8\sum}\rho_{b-c}\left(\frac{4(1-\nu_b^2)}{E_b}+\frac{4(1-\nu_c^2)}{E_c}\right)\right]^{1/3},$$
$$b=\eta\left[\frac{3P}{8\sum}\rho_{b-c}\left(\frac{4(1-\nu_b^2)}{E_b}+\frac{4(1-\nu_c^2)}{E_c}\right)\right]^{1/3} \tag{5}$$

where $\xi$ and $\eta$ are the coefficients of $a$ and $b$, and can be calculated as follows:

$$\begin{cases}\cos\tau=\left[(2-e^2)E\left(e,\frac{\pi}{2}\right)-2(1-e^2)K\left(e,\frac{\pi}{2}\right)\right]/\left[e^2E\left(e,\frac{\pi}{2}\right)\right]\\ \xi=\left\{2E\left(e,\frac{\pi}{2}\right)/\left[\pi(1-e^2)\right]\right\}^{1/3},\ \eta=\left[2\sqrt{1-e^2}E\left(e,\frac{\pi}{2}\right)/\pi\right]^{1/3},\ \vartheta=2K\left(e,\frac{\pi}{2}\right)/(\pi\xi)\end{cases} \tag{6}$$

where $\cos\tau$ is the main curvature function, as to the contacts between the ball and the raceways of the carriage and rail, they are $\cos\tau_{b-c}=\left(|\rho_{bI}-\rho_{bII}|+|\rho_{cI}-\rho_{cII}|\right)/(\sum\rho_{b-c})$ and $\cos\tau_{b-r}=\left(|\rho_{bI}-\rho_{bII}|+|\rho_{rI}-\rho_{rII}|\right)/\sum\rho_{b-r}$, $e$ is the eccentricity of the contact ellipse, and $K(e,\pi/2)$ and $E(e,\pi/2)$ are the complete elliptic integrals of the first kind and second kind, respectively

$$K\left(e,\frac{\pi}{2}\right)=\int_0^{\frac{\pi}{2}}\left(1-e^2\sin^2\Phi\right)^{-\frac{1}{2}}d\Phi,\quad E\left(e,\frac{\pi}{2}\right)=\int_0^{\frac{\pi}{2}}\left(1-e^2\sin^2\Phi\right)^{\frac{1}{2}}d\Phi \tag{7}$$

A MATLAB script was written to solve Eq. (6). Here, once the auxiliary value $\cos\tau_{b-c}$ or $\cos\tau_{b-r}$ is determined, $e$ can be solved by inverse analysis, and then $\xi$, $\eta$ and $\vartheta$ are obtained. For example, for the radius of the ball and the raceway groove of the carriage

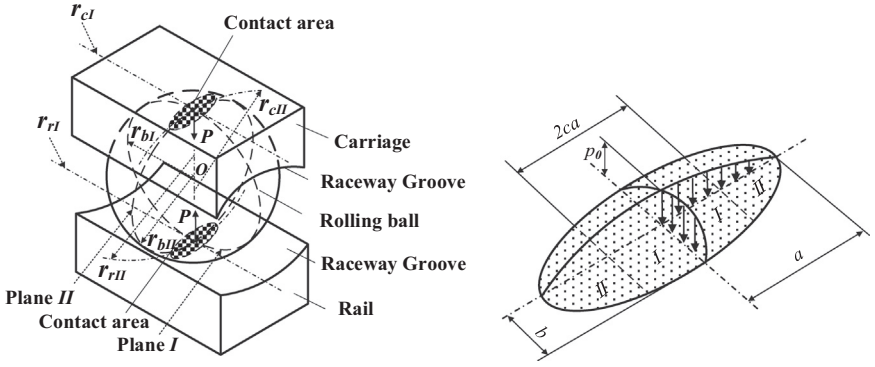


**Fig. 1.** Geometry of contacting bodies and contact ellipse.